

TIPP 2011 - Technology and Instrumentation in Particle Physics

Silicon sensor technologies for the ATLAS IBL upgrade

P. Grenier^{a*}, on behalf of the ATLAS IBL, PPS and 3D Collaborations

^a*SLAC National Accelerator Laboratory, Menlo Park, CA94025, USA*

Abstract

An overview of radiation hard planar and 3D pixel sensor technologies currently under development for ATLAS upgrades is presented. The first upgrade will be the installation in 2013 of an additional pixel layer inside the current Detector, the Insertable B Layer (IBL). The two technologies are competing to equip the IBL. The IBL sensor qualification procedure is described. Beam test results of un-irradiated and irradiated planar and 3D sensors are presented.

© 2012 Published by Elsevier B.V. Selection and/or peer review under responsibility of the organizing committee for TIPP 11. Open access under [CC BY-NC-ND license](https://creativecommons.org/licenses/by-nc-nd/4.0/).

Keywords: ATLAS Upgrade and Insertable B layer; Silicon sensors, Radiation hard detectors.

1. Introduction

New pixel sensors are currently under development in ATLAS [1] for future upgrades. The first upgrade stage will consist in the construction of a new pixel layer that will be installed in the current Pixel Detector [2] during the 2013 LHC shutdown. The new layer (Insertable-B-Layer, IBL [3]) will be inserted between the innermost layer of the current Pixel Detector and the beam pipe at a radius of 3.2cm. The expected high radiation levels require the use of radiation hard technology for both the front-end chip and the sensor. Two different pixel sensor technologies are envisaged for the IBL. One option is developed by the ATLAS Planar Pixel Sensor (PPS) Collaboration and is based on classical silicon sensors where the electrodes are implanted on the surface of the wafer. Several designs are currently investigated: a) n-in-n design similar to current pixel sensors used in the current ATLAS Pixel Detector with large dead area at

* Email: grenier@slac.stanford.edu.

sensor edges due to guard rings, b) n-in-n design with slim edge and c) n-in-p design. The n-in-n slim-edge design is the option considered for the IBL. The other option is developed by the ATLAS 3D Collaboration. 3D silicon technology is an innovative combination of VLSI and MEMS (Micro-Electro-Mechanical-Systems) where electrodes are fabricated inside the silicon bulk instead of being implanted on the wafer surface. Two layouts have been developed: one with electrodes penetrating entirely the wafer thickness and with active edges (full-3D) and one with no active edges with electrodes do not necessarily penetrating the entire thickness (partial-3D). For IBL only the later design is considered. The IBL will either be equipped with 100% planar sensors or by 75% planar and 25% 3D sensors. In the later case the 3D sensors would be installed at the largest angles where the 3D technology would lead to better tracking resolution in the z direction. The final choice will occur in February 2012,

2. ATLAS Insertable B Layer

2.1. Plans for LHC and ATLAS upgrades

Three main LHC upgrades are currently planned or envisaged:

- Phase 0: 15 month shutdown in 2013-2014. The magnetic dipole network of the machine will be brought to full power (replacement of all inter-magnet splices), allowing to reach to the nominal beam energy of 7 TeV. ATLAS will use this opportunity to install the IBL (see below).
- Phase 1: currently planned to be a 12 month shutdown in 2017-2018. The machine will be able to reach an instantaneous luminosity of $1\text{-}2 \times 10^{34} \text{ cm}^{-2}\text{s}^{-1}$. By the end of Phase 1, the integrated luminosity should reach 300 fb^{-1} . The ATLAS forward muon detector and the data acquisition system should go minor upgrades.
- Phase 2: currently envisaged to a 18 month shutdown in 2021-2022. An instantaneous luminosity of $5 \times 10^{34} \text{ cm}^{-2}\text{s}^{-1}$ is targeted. ATLAS shall go through a major upgrade involving TDAQ, L1Trigger, Calorimeter electronics and full replacement of the inner tracker.

2.2. The ATLAS Insertable B Layer

The current ATLAS Pixel Detector is composed of three layers. There are two main motivations to add a fourth layer:

- a) Due to the large integrated doses and luminosity effect, some of the pixel modules are expected to fail leading to the degradation with time of the performance of the current innermost layer of the Pixel Detector, affecting in particular the b-tagging.
- b) The addition of a pixel layer at a smaller radius and therefore closer to the interaction point will help to improve the measurement of the tracks impact parameter.

Originally the plan was to replace the first layer of the current detector. The entire Inner Detector would have had to be completely removed from ATLAS. This was judged to be too risky and it was rather

decided to install an additional layer inside the current Pixel Detector. The IBL will be mounted on a new, smaller radius, beam pipe. The available space for the new layer is very small with an inner radius of 31mm and an outer radius of 40mm, see Fig 1. The IBL will consist of 14 staves, 64cm long, each loaded with 32 assemblies of silicon sensor bump bonded to the newly developed FE-14 radiation hard front-end chip [4]. The FE-14 chip is an array of 80 columns x 336 rows of $50\mu\text{m} \times 250\mu\text{m}$ pixel cells.

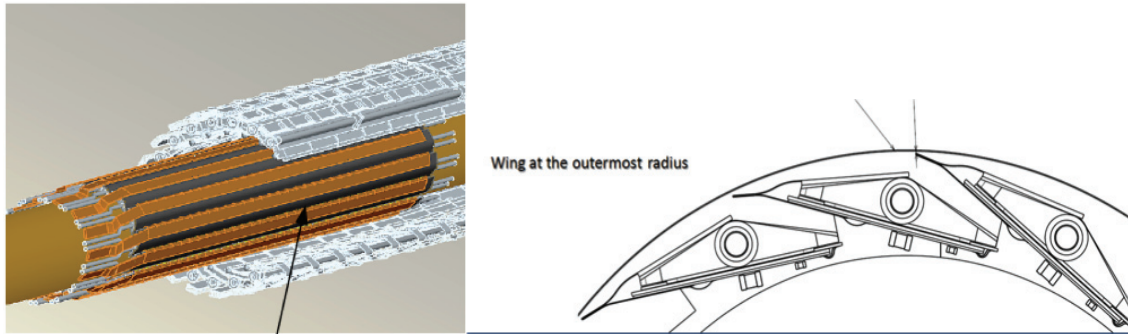


Fig. 1. (a) Insertion of the IBL, mounted on the beam pipe, inside the current Pixel Detector; (b) Cross section of IBL staves.

2.3. IBL sensor specifications, qualifications and production

The small IBL radius requires radiation hard sensors. Until replacement, the projected radiation doses, including safety factors are 250 Mrad of Total Ionizing Dose (TID) and $5 \cdot 10^{15} \text{ n}_{\text{eq}}/\text{cm}^2$ of Non Ionizing Energy Loss (NIEL). Besides radiation dose, the sensors are required to fulfill the following requirements:

- Maximum bias voltage: 1000V.
- Sensor thickness: $225 \pm 25 \mu\text{m}$.
- Coolant temperature: -30C .
- Sensor temperature: -15C .
- Maximum power dissipation $200\text{mW}/\text{cm}^2$ at -15C .
- Inactive edge width: $450\mu\text{m}$.
- Tracking efficiency greater than 98%.

The IBL installation was originally planned for the Phase 1 shutdown in 2017. However in January 2011, given the exceptional running performance of the machine, the Phase 0 shutdown initially planned

for 2012 was delayed to 2013 in order to let the LHC experiments accumulate a large amount of statistics and possibly reach one or more of the main physics goals of the LHC. This gave the opportunity to install the IBL in 2013 instead of the Phase 1 shutdown. However, this had a strong impact on the IBL schedule, in particular for the sensors for which all the final R&D and pre-production phases had to be entirely revisited in accordance to the new IBL overall schedule.

The two planar and 3D competing sensor technologies went from January to July 2011 through a fast track qualification with several irradiation campaigns and beam tests at DESY and CERN, and pre-production. A review panel met in July and recommended to equip the IBL with 75% of planar sensors in the low-medium η region and with 25% of 3D sensors in the large η region. The production of both sensors is expected to be completed by summer 2012, while the stave loading will start in March 2012. The planar modules will be produced as two-chip sensor tiles and 3D modules as single chip tiles, see Fig 2.

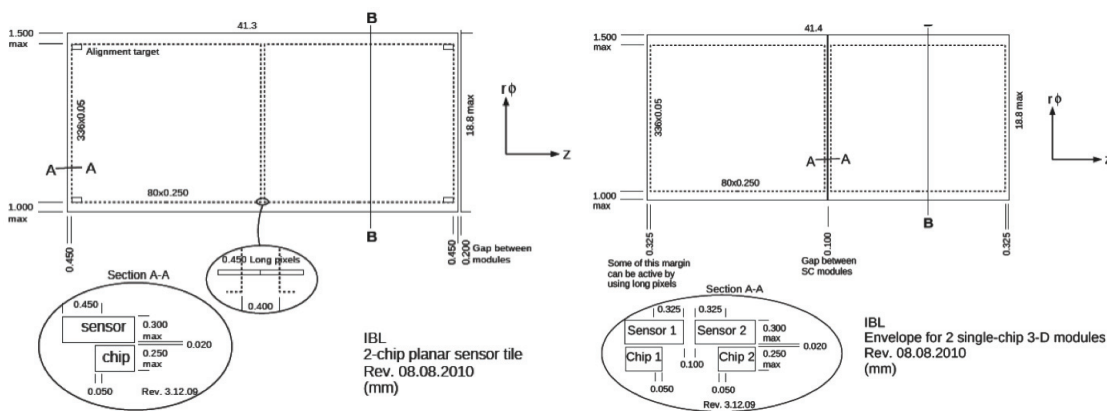


Fig. 2. (a) Planar two-chip sensor tile; (b) 3D 1-chip sensor tile.

3. Pixel sensor technologies for the IBL

Both sensor technologies are developed within ATLAS R&D Collaborations, the Planar Pixel Sensor (PPS) and the 3D Collaborations.

3.1. 3D Sensors

The original design of 3D sensor was proposed in 1997 [5]. Instead of being implanted on the surface of the wafer as in the case of planar sensor, electrodes are processed through the thickness of the wafer, see Fig 3. This had the main advantage of considerably reduce the distance between the electrodes. Typical inter-electrode distance is 50-80 μ m. Two different designs are being under investigation, although the later one was chosen for the IBL:

- a) full-3D where electrodes penetrate the entire thickness with active edge.
- b) Partial-3D where electrodes are processed from both sides of the wafer and do not penetrate the entire thickness, see Fig 3. Slim edge is achieved.

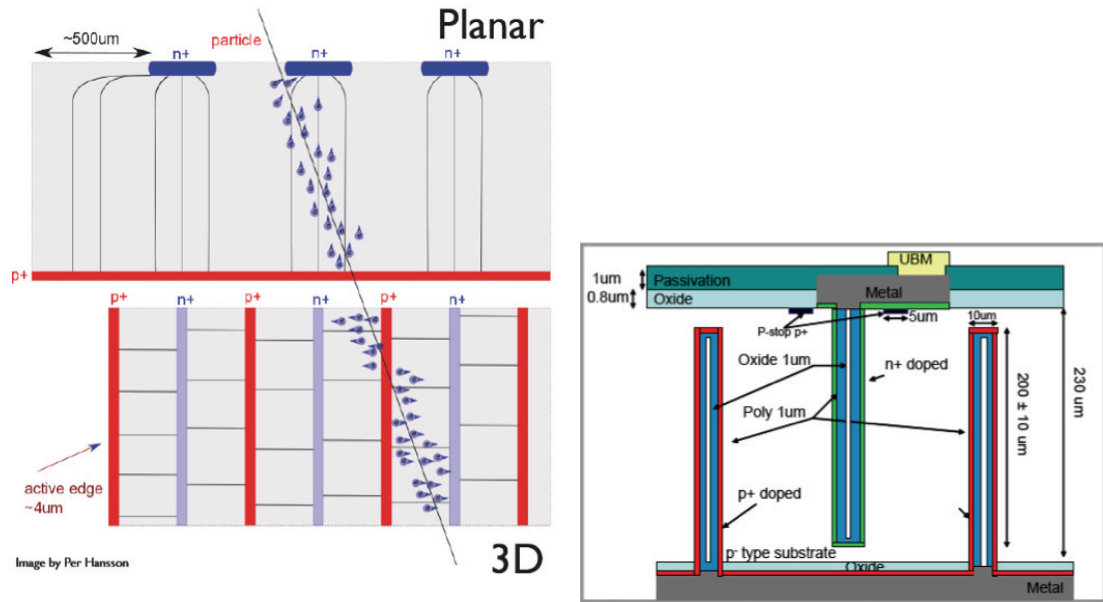


Fig. 3. (a) Principle of 3D sensors, comparing with Planar technology; (b) Principle of Partial-3D. Short inter-electrode distance ensures low depletion voltage and therefore low dissipated power, fast charge collection and smaller trapping probability therefore making radiation hard sensors. In case of full-3D, the sensor edge can be made an electrode, making the edge active. The complications are the slight loss of efficiency at normal incidence due to partially inactive columns and the production cost.

3.2. Planar Pixel Sensors

The PPS Collaboration has been doing developments on planar sensors in several areas: slim edges, bulk material, simulation of sensor design and detector layout, low threshold operation of front-end readout, low cost and large scale production, and the most important, radiation hardness.

The advantages of planar sensors are well known: mature technology requiring standard processing, low production cost and high yield and experience from current ATLAS Pixel Detector. The main challenge is operation after high radiation dose which will require high bias voltage and efficient cooling.

Three designs had been envisaged for the IBL:

1. Conservative n-in-n design, very similar to the sensors used in the current ATLAS Pixel Detector.
2. Slim edge n-in-n design ($\sim 200\mu\text{m}$ inactive region).
3. Thin ($\sim 150\mu\text{m}$ thickness) n-in-p sensors.

For the IBL, the choice was the slim edge design as it provided a compromise between radiation hardness, matured development and inactive region between modules. The slim edge design is shown in

Fig 4: it combines longer (500 μm) edge pixels and guard rings shifted underneath the active pixel region. For comparison, the conservative design with 450 μm inactive region is also shown.

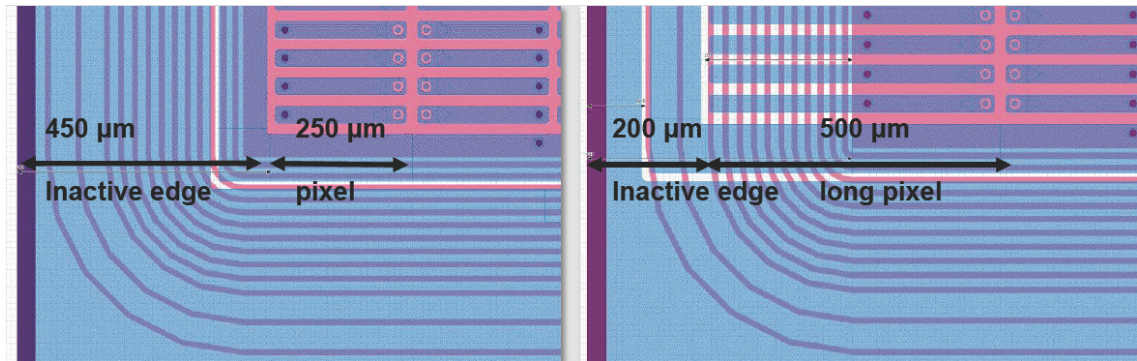


Fig. 4. (a) Planar Conservative design; (b) Planar Slim Edge design.

4. Testbeam measurements

Results presented here were obtained from two beam tests at DESY in February and April 2011 using 4 GeV electrons from the DESYII Synchrotron machine. The high resolution EUDET [6] telescope was used for track measurement. The telescope consisted of two arms of three Mimosas22 pixel sensors which is an array of 576 x 1172 pixels with a pitch of 18.6 μm covering an active area of 10.6 x 21.2 mm^2 . Typical trigger rate was 300Hz during normal operation.

Devices Under Test (DUT) were installed between the two telescope arms. In order to reduce effects of multiple scattering only two DUTs were installed at a time, a reference sensor and the actual device under test.

The deposited charge was estimated in terms of digital time-over-threshold (TOT) measured in units of the LHC bunch crossing rate 25ns. Front-end charge thresholds and TOT to charge conversion were tuned separately for each sample, depending if it was a planar or a 3D sensor and if it was irradiated or not. Below are the TOT and tracking efficiency measurements for three of the samples tested at DESY. The tracking efficiency is determined by extrapolating tracks from the telescope to the DUT where we check for a matching hit. All results are for data taken with the beam impinging the sensor at normal incidence.

4.1. Results of un-irradiated Slim Edge Design PPS sensor

This sample was the very first FE-I4 sensor tested in the beam. The threshold was set at 3200e⁻ and the TOT to Charge conversion was tuned for 10TOT@30ke⁻. Fig 5 shows the TOT distribution and the

tracking efficiency map where the efficiency is checked for each pixel over the entire sensor area. To avoid fake tracks, a hit in the reference sensor is required.

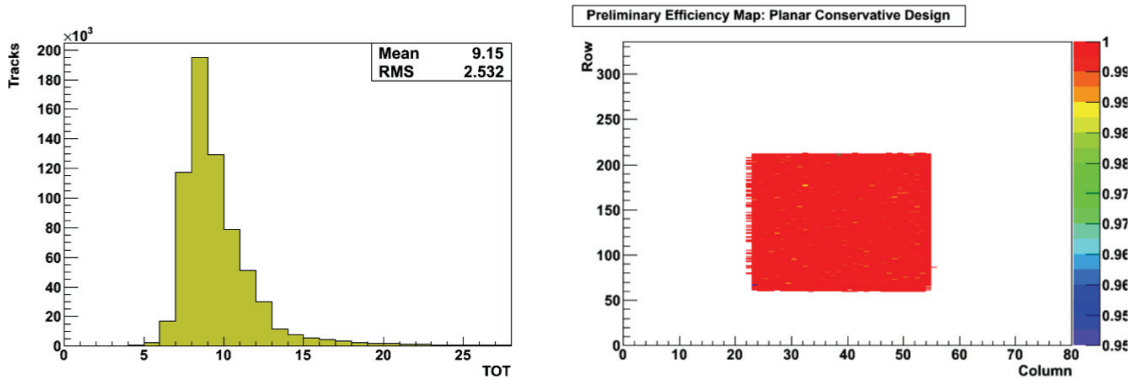


Fig. 5. Un-irradiated Slim Edge Design PPS sensor (a) Cluster TOT distribution; (b) Tracking efficiency map.

The overall efficiency for this sensor is 99.95% ,which is excellent.

4.2. Results of irradiated Conservative Design PPS sensor

This is the first measurement of an irradiated FE-I4 planar sensor, with $250\mu\text{m}$ thickness and conservative design. This sample has been irradiated with reactor neutrons at $4.10^{15} \text{ n}_{\text{eq}}/\text{cm}^2$. Fig 6 shows the TOT distribution and the tracking efficiency map. The bias voltage was -1000V and the sensors were cooled down using dry ice.

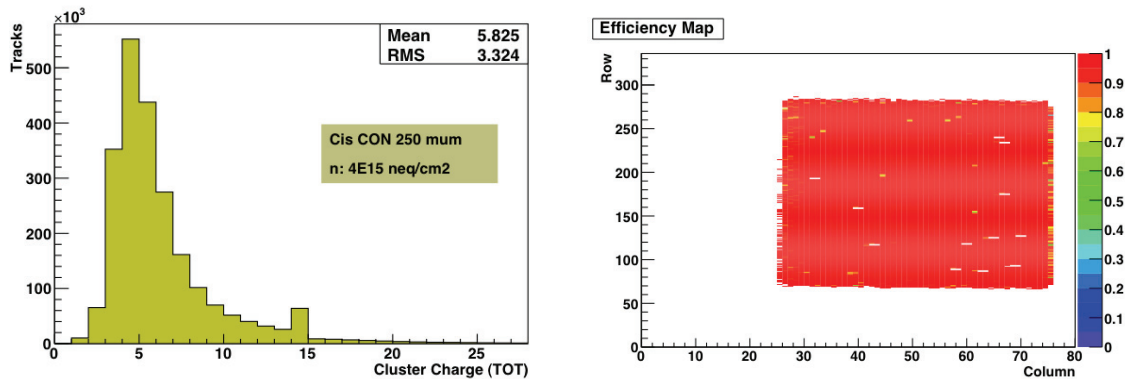


Fig. 6. Irradiated Conservative Design sensor (a) Cluster TOT distribution; (b) Tracking efficiency map.

The charge collection efficiency is greater than 50% and the overall efficiency for this sensor is 98.4%. Some dead pixels can be seen in the efficiency map.

4.3. Results of un-irradiated 3D sensor

This sample was the very first FE-I4 3D sensor tested in the beam. The threshold was set at 3200e- and the TOT to Charge conversion was tuned for 10TOT@20ke-. Fig 7 shows the TOT distribution and the tracking efficiency map.

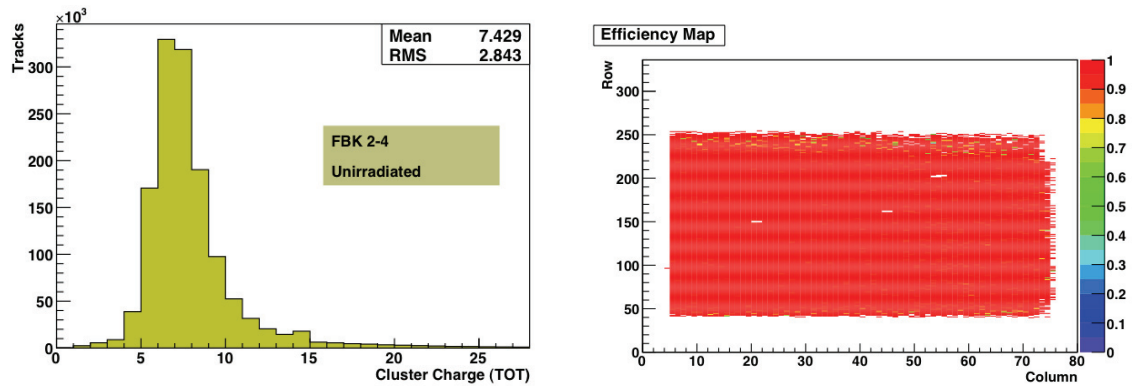


Fig. 7. Un-irradiated 3D sensor (a) TOT distribution; (b) Tracking efficiency map.

The overall efficiency for this sensor is 98%. Some of the tracking efficiency is lost due to tracks going through the electrodes. Electrodes are not filled and therefore do not produce charge.

5. Conclusion

New pixel sensor technologies are under development for ATLAS upgrades. Planar and 3D sensors are competing to equip the Insertable B layer that will be installed in the detector in 2013. The two technologies went in 2011 through a heavy program of irradiations and beam tests. The first beam test results have been presented in this contribution. References

- [1] The ATLAS Collaboration, “The ATLAS experiment at the CERN Large Hadron Collider”, 2008, JINST 3 S08003.
- [2] G. Add et al, “ATLAS Pixel Detector electronics and sensors”, 2008, JINST 3 P0700
- [3] ATLAS Collaboration, ATLAS TDR 19, CERN-LHCC-2010-013.
- [4] M. Garcia-Sciveres *et al*, NIM A 636, (2011) 155.
- [5] S. Parker, J. Segal and C. Kenney, NIM A395 (1997) 328.
- [6] D. Haas, in: Proceedings of the LCWS2007, 2007, <thhp://www.eudet.org>